Available online at www.sciencedirect.com
ScienceDirect
Journal of the European Ceramic Society 30 (2010) 3435–3443
www.elsevier.com/locate/jeurceramsoc

Preparation of alkaline-earth titanates by accelerated solid-state reaction in water vapor atmosphere

Takahiro Kozawa, Ayumu Onda, Kazumichi Yanagisawa *

Research Laboratory of Hydrothermal Chemistry, Faculty of Science, Kochi University, 2-5-1 Akebono-cho, Kochi 780-8520, Japan

Received 15 February 2010; received in revised form 2 July 2010; accepted 16 July 2010
Available online 14 August 2010

Abstract

Alkaline-earth titanates, $MTiO_3$ (M = Mg, Ca, Sr and Ba), were prepared by solid-state reactions in air and water vapor atmospheres to investigate the effects of water vapor on the formation of $MTiO_3$. The formation of $MTiO_3$ was accelerated more or less by water vapor. Acceleration effect by water vapor increased in the following order: $MgTiO_3$ and $CaTiO_3 \ll SrTiO_3 < BaTiO_3$. The formation of $SrTiO_3$ and $BaTiO_3$ was drastically accelerated by water vapor even though the coarse particles of $SrCO_3$ and $BaCO_3$ remained in the starting mixtures. The difference in its effect might be mainly attributed to the vapor pressure of $M(OH)_2$. Gas-phase transport of $M(OH)_2$ would become important for the formation of $MTiO_3$ by solid-state reactions in water vapor atmosphere.

Keywords: Powders-solid-state reaction; $BaTiO_3$ and titanates; Water vapor

1. Introduction

Alkaline-earth titanates ($MTiO_3$, M = Mg, Ca, Sr and Ba) are important materials for the electronic industry. $MgTiO_3$ has an ilmenite structure and the others have a perovskite structure. Among these titanates, $BaTiO_3$ is the most widely used because of its high dielectric constant, ferroelectric properties and positive temperature coefficient of electrical resistivity.[1] $BaTiO_3$ and other titanates have been usually synthesized by the high temperature solid-state reaction between TiO_2 and each alkaline-earth carbonate. The high calcination temperature required in this process leads to many disadvantages of the calcined powders, such as large particle size with a wide size distribution and high degree of particle agglomeration.[2] Therefore, current research efforts have been focused on the reduction of particle size of raw materials to submicrometer or even to nanoscale in order to decrease the calcination temperature.[3–6] In addition, mechanochemical effects are known to be quite effective to decrease the calcination temperature for solid-state reaction to prepare $BaTiO_3$,[7–10] $MgTiO_3$,[11] $CaTiO_3$[12] and $SrTiO_3$.[13]

On the other hand, we have previously shown that the formation of $BaTiO_3$ and β-Ca_2SiO_4 by solid-state reactions is drastically accelerated by water vapor without particular mechanochemical processing.[14,15] The solid-state reaction process in water vapor atmosphere should be effective to prepare other ceramic powders consisting of oxygen polyhedra at low temperatures. In this paper, we applied this method to the preparation of $MgTiO_3$, $CaTiO_3$, $SrTiO_3$ and $BaTiO_3$ and investigated the effects of water vapor on the formation of $MTiO_3$. Special attention was given to the gas-phase transport of the reactant in water vapor atmosphere.

2. Experimental procedures

The raw materials used were commercially available $Mg_5(CO_3)_4(OH)_2{\cdot}4H_2O$ (S_{BET} = 20.93 m^2/g, d_{BET} = 0.13 μm), $CaCO_3$ (S_{BET} = 5.63 m^2/g, d_{BET} = 0.40 μm), $SrCO_3$ (S_{BET} = 4.21 m^2/g, d_{BET} = 0.38 μm), $BaCO_3$ (S_{BET} = 1.68 m^2/g, d_{BET} = 0.83 μm) and TiO_2 (rutile, S_{BET} = 5.60 m^2/g, d_{BET} = 0.25 μm) with a trace of anatase phase. Starting powders with stoichiometric $MgTiO_3$, $CaTiO_3$, $SrTiO_3$ and $BaTiO_3$ composition were mixed in a dry condition for 6 h with 280 rpm using stainless jars and media. The mixed powders (0.3 g each) placed in an alumina boat were calcined at various temperatures for 2 h in air and water vapor atmospheres by a

* Corresponding author. Tel.: +81 88 844 8352; fax: +81 88 844 8362.
E-mail address: yanagi@kochi-u.ac.jp (K. Yanagisawa).

0955-2219/$ – see front matter © 2010 Elsevier Ltd. All rights reserved.
doi:10.1016/j.jeurceramsoc.2010.07.027

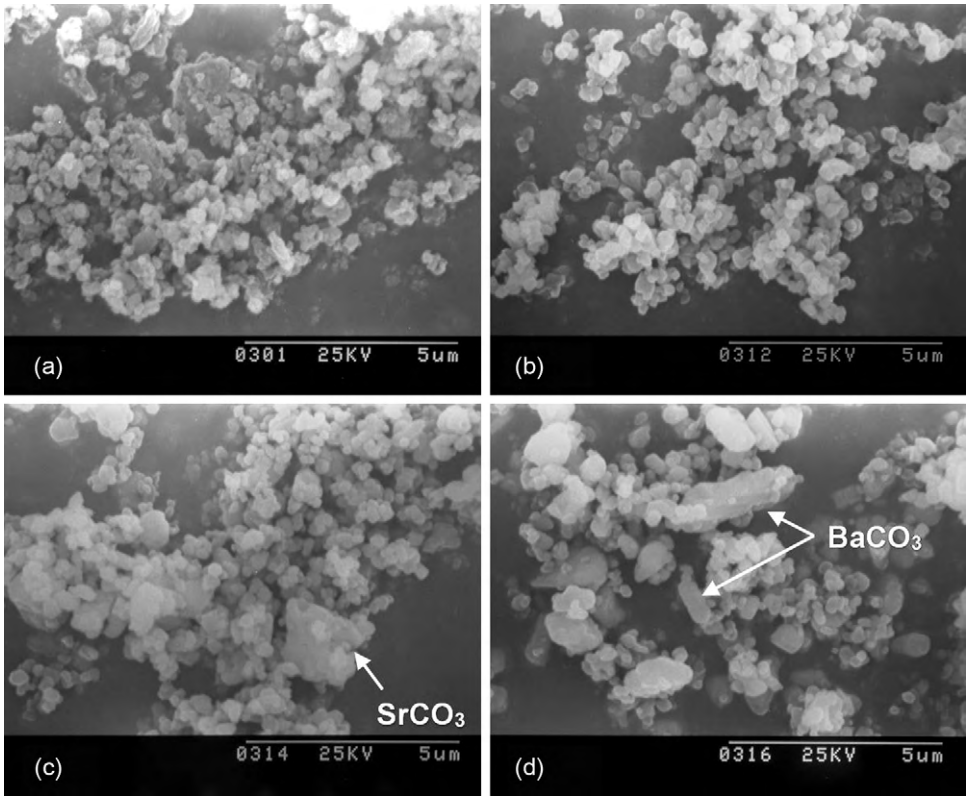

Fig. 1. SEM photographs of the starting mixtures before calcination: (a) $Mg_5(CO_3)_4(OH)_2{\cdot}4H_2O$–$TiO_2$, (b) $CaCO_3$–TiO_2, (c) $SrCO_3$–TiO_2 and (d) $BaCO_3$–TiO_2.

tubular furnace equipped with a water evaporator. For water vapor atmosphere, distilled water was introduced at a flow rate of 2 mL/min into the evaporator without a carrier gas to generate 100% water vapor atmosphere in the furnace. Calcinations in air atmosphere were performed in stagnant condition in the same furnace by removing the evaporator. In a previous paper, we examined the effect of forcible removing of CO_2 gas from the reaction field on the formation of $BaTiO_3$, and concluded that N_2 gas flow for forcible removing of CO_2 gas had little effects on the decomposition of $BaCO_3$.[14] Consequently, we investigated the effects of water vapor atmosphere on the formation of $MTiO_3$ comparing with that in stagnant air atmosphere.

Powder X-ray diffractions (XRD) were measured on a Rigaku Rotaflex RAD-RC diffractometer operating at 40 kV and 100 mA using Cu Kα radiation. The patterns were col-

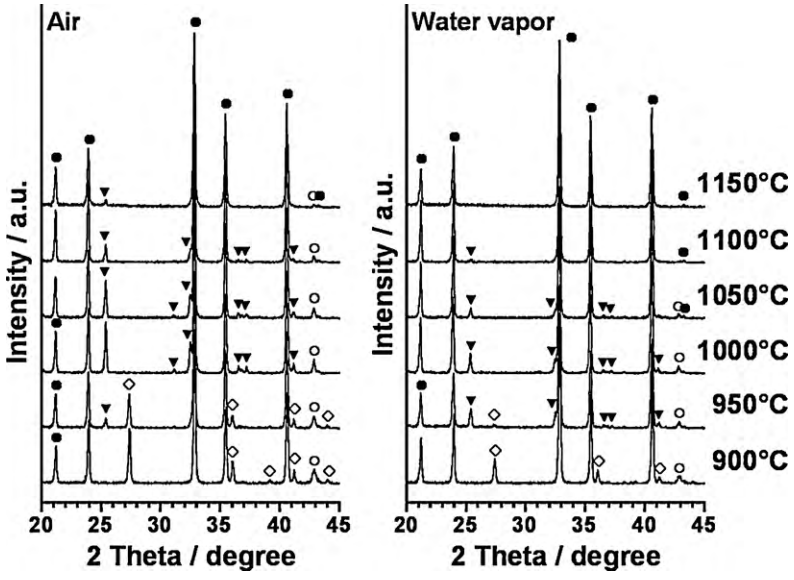

Fig. 2. XRD patterns of the samples obtained by solid-state reactions between $Mg_5(CO_3)_4(OH)_2{\cdot}4H_2O$ and TiO_2 in air and water vapor atmospheres at 900–1150 °C for 2 h. (●) $MgTiO_3$, (▼) $MgTi_2O_5$, (◊) rutile TiO_2, (◯) MgO.

lected in the range of 5–80° in $2\theta/\theta$ scanning mode with a 0.02° step and scanning speed of 4°/min. The amount of each crystalline phase was estimated by semi-quantitative analysis from XRD peak areas of the most intense peak of each compound, except for $BaTiO_3$. Reacted fraction (α) of each compound was defined as a ratio of the strongest peak area of the compound against the total of the strongest peak area of all compounds formed in sample. The amount of $BaTiO_3$ was determined by quantitative analysis of XRD using the internal standard method.[14] Specific surface area, S_{BET}, was measured by the BET method using N_2 with a Yuasa-ionics NOVA-1200 instrument. The equivalent BET diameter, d_{BET}, was calculated by the equation: $d_{BET} = 6/(\rho \cdot S_{BET})$, where ρ is the density of $Mg_5(CO_3)_4(OH)_2 \cdot 4H_2O$ 2.26 g/cm^3, $CaCO_3$ 2.71 g/cm^3, $SrCO_3$ 3.79 g/cm^3, $BaCO_3$ 4.31 g/cm^3 and rutile type TiO_2 4.25 g/cm^3. Micrographs of scanning electron microscopy (SEM) were obtained by using Hitachi S-530 electron microscope operating at 25 kV.

3. Results and discussion

3.1. Characterization of starting mixtures

Fig. 1 shows the SEM photographs of starting mixtures prepared by ball milling for 6 h. Starting mixtures of $Mg_5(CO_3)_4(OH)_2 \cdot 4H_2O$–$TiO_2$ and $CaCO_3$–TiO_2 had relatively high homogeneity. In contrast, coarse particles of $SrCO_3$ and $BaCO_3$ remained in those of $SrCO_3$–TiO_2 and $BaCO_3$–TiO_2, respectively.

3.2. Formation of $MgTiO_3$

Fig. 2 shows the XRD patterns of the samples obtained by solid-state reactions between $Mg_5(CO_3)_4(OH)_2 \cdot 4H_2O$ and TiO_2 in air and water vapor atmospheres at 900–1150 °C for 2 h. In both atmospheres, $Mg_5(CO_3)_4(OH)_2 \cdot 4H_2O$ was already decomposed below 600 °C to form $MgTiO_3$ and MgO. As shown in Fig. 2, the major phase of the calcined samples was $MgTiO_3$ in both atmospheres when the starting mixtures were calcined at 900 °C for 2 h. On the other hand, the minor phase, $MgTi_2O_5$, was obtained at 950 °C and the amount of $MgTi_2O_5$ increased simultaneously with disappearance of the TiO_2 phase. It has been reported that $MgTi_2O_5$ has a pseudobrookite type structure with an orthorhombic unit cell[16] and is formed even by calcination of the oxide mixtures with 1:1 molar ratio.[17,18] The formed $MgTi_2O_5$ was reacted with residual MgO to form $MgTiO_3$ with increasing calcination temperature in both atmospheres. Single-phase $MgTiO_3$ was obtained by calcination at 1150 °C for 2 h in water vapor atmosphere, whereas the trace amounts of $MgTi_2O_5$ and MgO remained in air atmosphere. In air atmosphere, calcinations at 1150 °C for 4 h or 1200 °C for 2 h were required to get a single-phase $MgTiO_3$.

Fig. 3 shows the reacted fraction of the $MgTiO_3$ and $MgTi_2O_5$ phases in both atmospheres. Formation of $MgTiO_3$ already started at 600 °C. The reacted fraction of the $MgTiO_3$ phase gradually increased up to 950 °C and 900 °C in air and water vapor atmospheres, respectively, and stayed constant because of

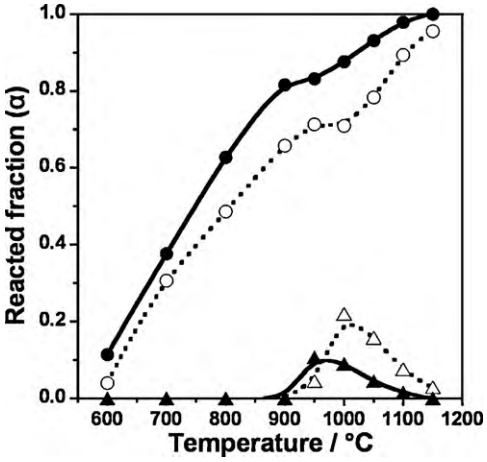

Fig. 3. Reacted fraction of the crystalline phases obtained by solid-state reactions between $Mg_5(CO_3)_4(OH)_2 \cdot 4H_2O$ and TiO_2 in air and water vapor atmospheres. Circles and triangles correspond to $MgTiO_3$ and $MgTi_2O_5$, and open and solid symbols correspond to air and water vapor atmospheres, respectively.

the formation of minor $MgTi_2O_5$ phase. After that, the amount of $MgTiO_3$ increased again with decrease of the $MgTi_2O_5$ phase. It is worth noting that the amount of $MgTi_2O_5$ obtained in water vapor atmosphere is half compared with that obtained in air atmosphere. Water vapor suppressed the formation of the intermediate phase.

On the basis of the results of XRD patterns (Fig. 2) and semi-quantitative analysis (Fig. 3), solid-state reaction between MgO and TiO_2 to form $MgTiO_3$ is shown as follows:

$$MgO + TiO_2 \rightarrow MgTiO_3 \quad (1)$$

$$MgTiO_3 + TiO_2 \rightarrow MgTi_2O_5 \quad (2)$$

$$MgTi_2O_5 + MgO \rightarrow 2MgTiO_3 \quad (3)$$

The formation of $MgTiO_3$ by solid-state reaction of MgO with TiO_2 (Eq. (1)) was accelerated by water vapor. Water vapor is considered to attack Ti–O–Ti bonds of rutile TiO_2 particle surface to promote rotation and movement of TiO_6 octahedra. Thus, MgO which has already formed by the decomposition of $Mg_5(CO_3)_4(OH)_2 \cdot 4H_2O$ easily reacts with TiO_6 octahedra to form $MgTiO_3$ up to 900 °C. As shown in Eq. (2), the intermediate $MgTi_2O_5$ phase would be formed by the reaction of $MgTiO_3$ with TiO_2, because the XRD peak intensity of MgO was not decreasing at 950 °C (Fig. 2). Furthermore, we also confirmed by solid-state synthesis of $MgTi_2O_5$ from $Mg_5(CO_3)_4(OH)_2 \cdot 4H_2O$ and TiO_2 that the reaction products up to 900 °C consisted of the $MgTiO_3$ and TiO_2 phases, and then $MgTiO_3$ was reacted with residual TiO_2 to form $MgTi_2O_5$ as the reaction advanced. In the case of the solid-state synthesis of $MgTiO_3$, the formation of intermediate $MgTi_2O_5$ phase was suppressed in water vapor atmosphere, because the reaction in Eq. (1) was accelerated by water vapor and consequently the amount of TiO_2 to form $MgTi_2O_5$ decreased.

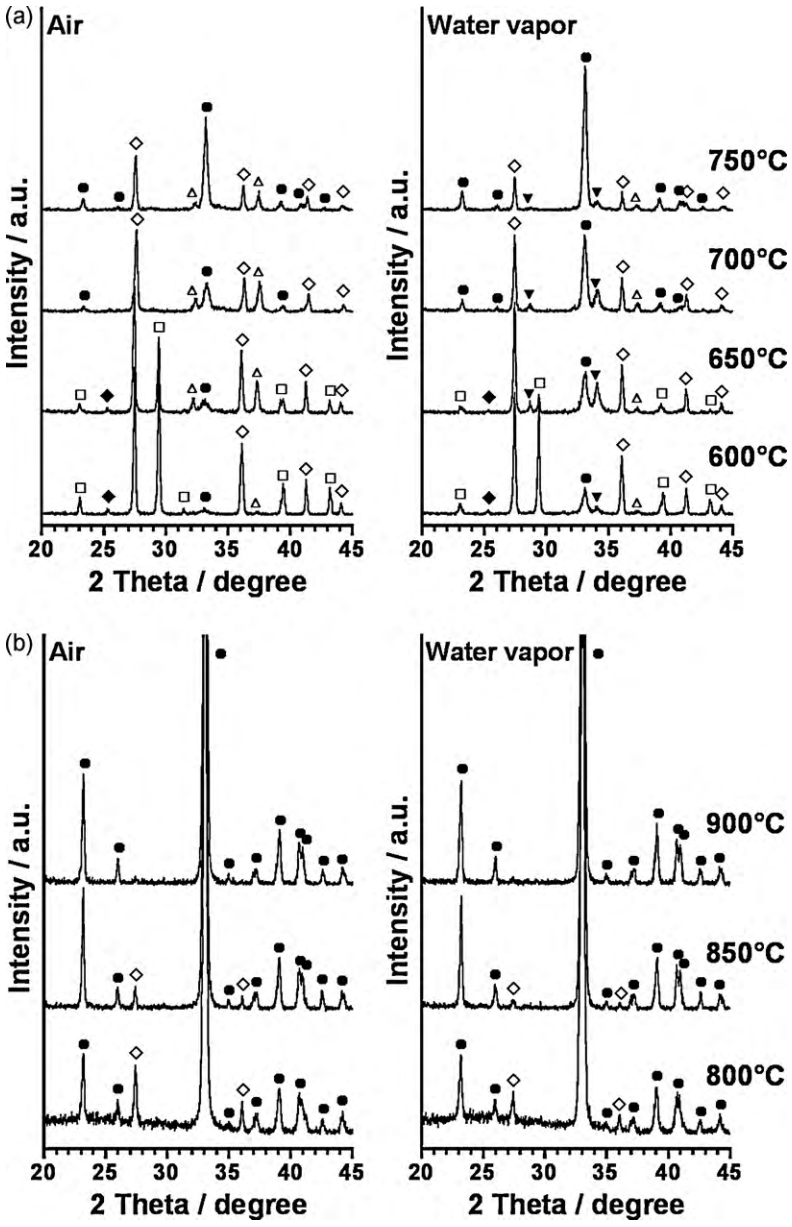

Fig. 4. XRD patterns of the samples obtained by solid-state reactions between $CaCO_3$ and TiO_2 in air and water vapor atmospheres at (a) 600–750 °C and (b) 800–900 °C for 2 h. (●) $CaTiO_3$, (◊) rutile TiO_2, (♦) anatase TiO_2, (□) $CaCO_3$, (△) CaO, (▼) $Ca(OH)_2$.

3.3. Formation of $CaTiO_3$

Fig. 4 shows the XRD patterns of the samples obtained by solid-state reactions between $CaCO_3$ and TiO_2 in air and water vapor atmospheres. A small amount of anatase was detected in the samples obtained in both atmospheres up to 650 °C and then disappeared by calcination at 700 °C (Fig. 4a). Anatase, a contaminant of the starting rutile, was transformed to rutile at around 700 °C. In air atmosphere, $CaCO_3$ remained in large quantities up to 650 °C, though the decomposition of $CaCO_3$ and formation of $CaTiO_3$ started at 600 °C. In contrast, in water vapor atmosphere, thermal decomposition of $CaCO_3$ and formation of $CaTiO_3$ were accelerated by water vapor. $Ca(OH)_2$ was detected because of the hydration of CaO during the cooling process of the sample in water vapor atmosphere.

The results shown in Fig. 4a clearly indicated that water vapor accelerated the thermal decomposition of $CaCO_3$ and then a large amount of $CaTiO_3$ was formed at lower temperatures than in air atmosphere. It has been shown that the thermal decomposition of $CaCO_3$ is accelerated by water vapor.[19–22] Wang and Thomson[21] described that adsorbed water vapor weakened Ca–CO_3 bond and the thermal decomposition of $CaCO_3$ was accelerated by water vapor. Furthermore, the lower CO_2 partial pressure in water vapor atmosphere might enhance the decomposition of $CaCO_3$. Therefore, it is concluded that the formation of $CaTiO_3$ in water vapor atmosphere was promoted by accelerated decomposition of $CaCO_3$ at low temperatures.

Fig. 4b shows the XRD patterns of the samples obtained by calcinations at high temperature region from 800 °C to 900 °C

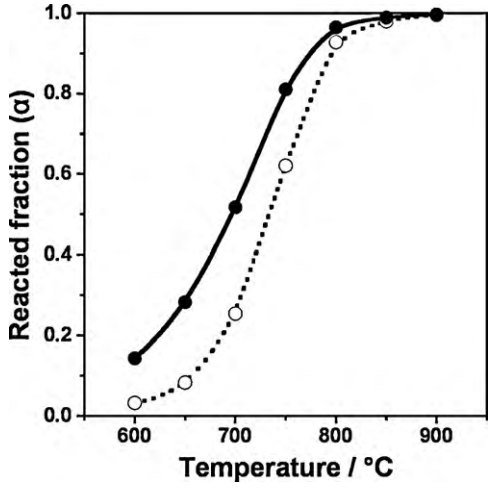

Fig. 5. Reacted fraction of the $CaTiO_3$ phase obtained by solid-state reactions between $CaCO_3$ and TiO_2 in (◯) air and (●) water vapor atmospheres.

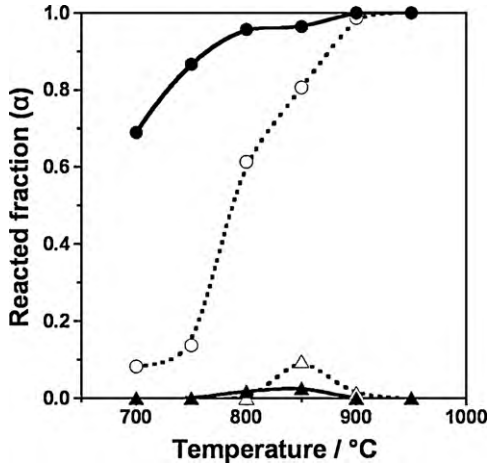

Fig. 7. Reacted fraction of the crystalline phases obtained by solid-state reactions between $SrCO_3$ and TiO_2 in air and water vapor atmospheres. Circles and triangles correspond to $SrTiO_3$ and $Sr_3Ti_2O_7$, and open and solid symbols correspond to air and water vapor atmospheres, respectively.

for 2 h. Formation of the single-phase $CaTiO_3$ required calcination at 900 °C in both atmospheres.

Fig. 5 shows the reacted fraction of the $CaTiO_3$ phase. In water vapor atmosphere, the amount of $CaTiO_3$ started to increase at low temperatures by accelerated decomposition of $CaCO_3$. However, the effect of water vapor became smaller at high temperatures.

3.4. Formation of $SrTiO_3$

Fig. 6 shows the XRD patterns of the samples obtained by solid-state reactions between $SrCO_3$ and TiO_2 in air and water vapor atmospheres at 700–950 °C for 2 h. In air atmosphere, $SrCO_3$ and TiO_2 remained in large quantities up to 850 °C. An intermediate phase, $Sr_3Ti_2O_7$, was detected after calcination at 850 °C and remained up to 900 °C. $Sr_3Ti_2O_7$ has a Ruddlesden–Popper structure building up from perovskite-like blocks.[23] Formation of the single-phase $SrTiO_3$ required calcination at 950 °C for 2 h in air atmosphere. In contrast, the thermal decomposition of $SrCO_3$ and formation of $SrTiO_3$ were accelerated by water vapor, and the single-phase $SrTiO_3$ was obtained at 900 °C for 2 h in water vapor atmosphere.

Fig. 7 shows the reacted fraction of the $SrTiO_3$ and $Sr_3Ti_2O_7$ phases in both atmospheres. The formation of $SrTiO_3$ was drastically accelerated by water vapor and $SrTiO_3$ was obtained in water vapor atmosphere at lower temperatures compared with in air atmosphere. In addition, the amount of $Sr_3Ti_2O_7$ was remarkably small in water vapor atmosphere.

On the basis of the results of XRD (Fig. 6) and semi-quantitative analysis (Fig. 7), solid-state reaction between

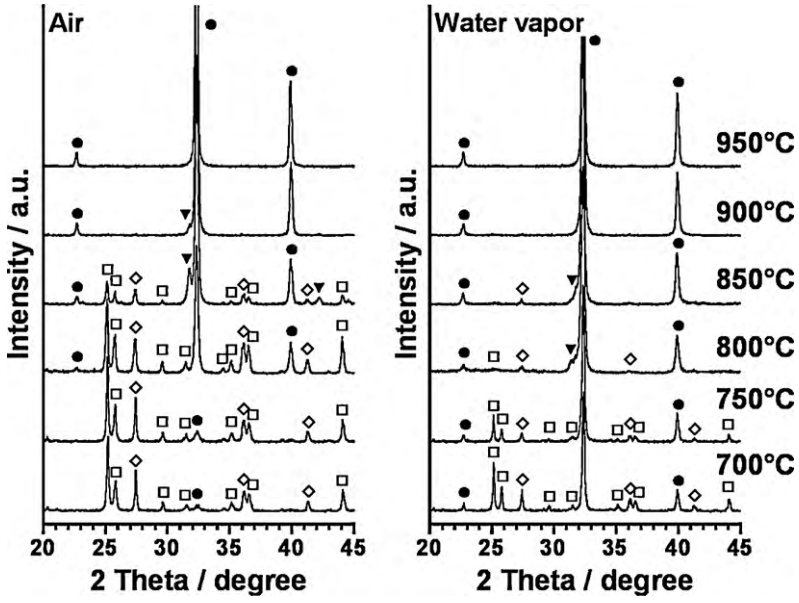

Fig. 6. XRD patterns of the samples obtained by solid-state reactions between $SrCO_3$ and TiO_2 in air and water vapor atmospheres at 700–950 °C for 2 h. (●) $SrTiO_3$, (▼) $Sr_3Ti_2O_7$, (◊) rutile TiO_2, (□) $SrCO_3$.

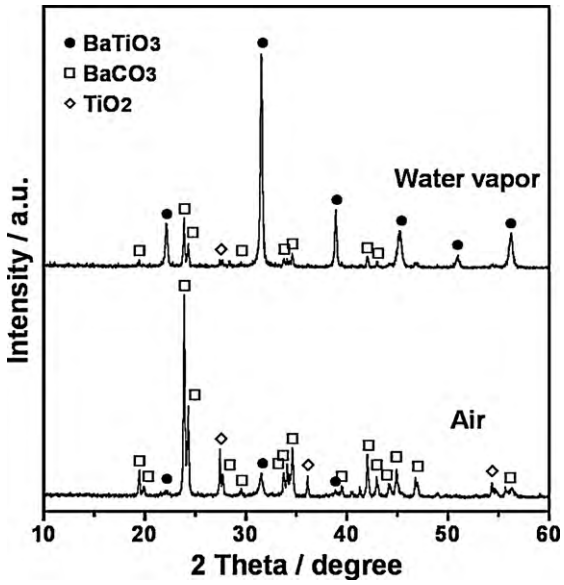

Fig. 8. XRD patterns of the samples obtained by solid-state reactions between $BaCO_3$ and TiO_2 in air and water vapor atmospheres at 700 °C for 2 h.

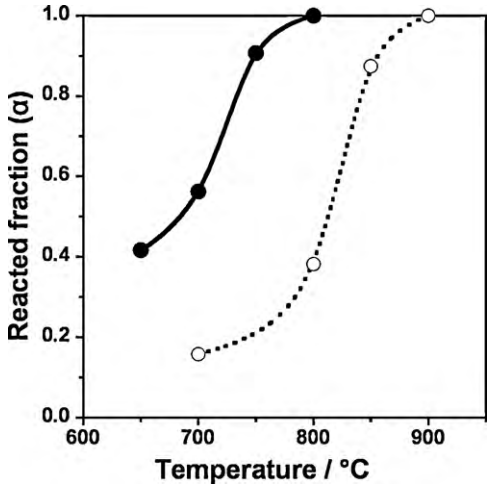

Fig. 9. Reacted fraction of the $BaTiO_3$ phase obtained by solid-state reactions between $BaCO_3$ and TiO_2 in (◯) air and (●) water vapor atmospheres.

$SrCO_3$ and TiO_2 to form $SrTiO_3$ is given as following:

$$SrCO_3 + TiO_2 \rightarrow SrTiO_3 + CO_2 \quad (4)$$

$$SrTiO_3 + 2SrCO_3 + TiO_2 \rightarrow Sr_3Ti_2O_7 + 2CO_2 \quad (5)$$

$$Sr_3Ti_2O_7 + TiO_2 \rightarrow 3SrTiO_3 \quad (6)$$

The formation of $SrTiO_3$ by solid-state reaction of $SrCO_3$ with TiO_2 (Eq. (4)) was accelerated by water vapor because of accelerated decomposition of $SrCO_3$, so that formation of the intermediate $Sr_3Ti_2O_7$ phase was suppressed. Liu et al.[24] showed that $SrTiO_3$ was formed at the initial stage of the molten salt synthesis of $Sr_3Ti_2O_7$ using $SrCO_3$, TiO_2 and KCl as raw materials, and then reacted with residual $SrCO_3$ and TiO_2 to form $Sr_3Ti_2O_7$. Therefore, the intermediate $Sr_3Ti_2O_7$ phase obtained in this study would be formed by the reaction as shown in Eq. (5).

3.5. Formation of $BaTiO_3$

We have already found that water vapor accelerated the formation of $BaTiO_3$ by solid-state reactions.[14] Fig. 8 shows the XRD patterns of the samples obtained by solid-state reactions between $BaCO_3$ and TiO_2 in air and water vapor atmospheres at 700 °C for 2 h. Water vapor accelerated the thermal decomposition of $BaCO_3$ and then $BaTiO_3$ started to form at low temperatures even from the starting mixture with coarse particles of $BaCO_3$ (Fig. 1d).

Fig. 9 shows the reacted fraction of the $BaTiO_3$ phase obtained by the XRD quantitative analysis with the internal standard method.[14] $BaTiO_3$ was formed by calcinations in water vapor atmosphere at temperatures 100–150 °C lower than those in air atmosphere. Thus, water vapor is fairly effective in this system.

3.6. Effect of water vapor on the formation of $MTiO_3$

The formation of alkaline-earth titanates was accelerated more or less by water vapor. However, the effects of water vapor on the formation of $MTiO_3$ phases differed considerably depending on alkaline-earth ions. Acceleration effect by water vapor increased in the following order: $MgTiO_3$ and $CaTiO_3 \ll SrTiO_3 < BaTiO_3$. Interestingly, the formation of $SrTiO_3$ and $BaTiO_3$ was accelerated by water vapor especially at low temperatures even though the coarse particle of $SrCO_3$ and $BaCO_3$ remained in the starting mixtures (Fig. 1). It is considered that water vapor has following effects to accelerate the formation of $MTiO_3$: (1) acceleration of MCO_3 decomposition, (2) acceleration of $MTiO_3$ formation by surface attacking of water vapor at the TiO_2 reaction front and by gas-phase transport of $M(OH)_2$ and (3) acceleration of solid-state diffusion of M^{2+} and O^{2-} ions in the $MTiO_3$ layer by formation of vacancies in the $MTiO_3$ structure.[14]

Actually, carbonates decomposition was accelerated by water vapor. However, the remained amount of $SrCO_3$ (Fig. 6) and the reacted fraction of the $SrTiO_3$ phase (Fig. 7) at 700 °C in water vapor atmosphere were comparable with those at 800 °C in air atmosphere. Thus, accelerated formation of $MTiO_3$ cannot be explained only by promotion of carbonates decomposition. The attacking of water vapor to TiO_2 was negligible to explain the difference of acceleration effects by water vapor, because the same starting TiO_2 powder was used in this study.

Many solid-state reactions are not actually solid–solid reactions but sometimes include gas-phase transport of the reactants. Gas-phase transport can occur by direct vaporization of the oxides or by formation of gaseous hydroxides, as observed in the systems $MgO–Al_2O_3$,[25] $NiO–Al_2O_3$,[26] $ZnO–Al_2O_3$[27] and $Gd_2O_3–Fe_2O_3$.[28] The formation of gaseous $Ba(OH)_2$ was previously proposed by Ubaldini et al.[29] to explain the more rapid formation of $BaZrO_3$ in humid air atmosphere than in dry air atmosphere. The volatility of alkaline-earth monoxides is greatly increased by the presence of water vapor because of the forma-

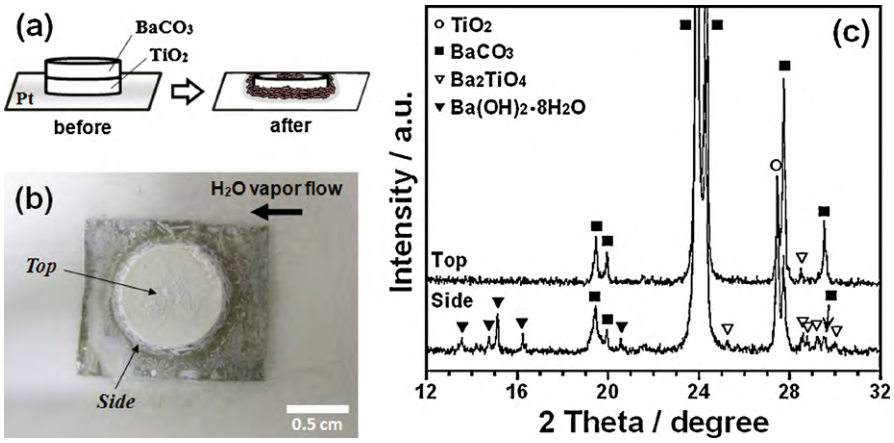

Fig. 10. (a) Schematic illustration of the superposed pellet of $BaCO_3$ and TiO_2 before and after calcination at 800 °C for 2 h in water vapor atmosphere. (b) Photograph and (c) XRD patterns of the pellet after calcination at 800 °C for 2 h in water vapor atmosphere.

tion of volatile hydroxide vapors given as follows:

$$MO(s) + H_2O(g) \rightarrow M(OH)_2(g) \quad (7)$$

The equilibrium constant K_p for the reaction in Eq. (7) could be expressed in terms of the partial pressure of alkaline-earth vapor species and water vapor as follows:

$$K_p = \frac{p(M(OH)_2)}{p(H_2O)} \quad (8)$$

where $p(H_2O)$ is 1 atm in water vapor atmosphere used this study. According to the thermodynamic data represented by L'vov[30] the vapor pressure of $Mg(OH)_2$ (g), $Ca(OH)_2$ (g), $Sr(OH)_2$ (g) and $Ba(OH)_2$ (g) is calculated to be 9.3×10^{-12} atm, 3.2×10^{-10} atm, 5.9×10^{-9} atm and 9.2×10^{-6} atm at 800 °C (1073 K), and 1.7×10^{-9} atm, 3.8×10^{-8} atm, 4.4×10^{-7} atm and 1.8×10^{-4} atm at 1000 °C (1273 K), respectively. These calculated values almost agree with estimated values by transpiration technique.[31–33] The vapor pressure of alkaline-earth hydroxides increases from $Mg(OH)_2$ to $Ba(OH)_2$, and this relationship is same as the order of accelerated effects of water vapor on the formation of $MTiO_3$. Moreover, the vapor pressure of $Ba(OH)_2$ is 3–6 orders of magnitude higher than the vapor pressure of the other hydroxides.

To verify the gas-phase transport of the reactant in water vapor atmosphere, separate calcination experiments were conducted by using the superposed pellets consisting of $BaCO_3$ and TiO_2 plane slab. The TiO_2 powders (0.15 g) were isostatically pressed at 100 MPa for 10 s, and then the $BaCO_3$ powders (0.15 g) were mounted on the TiO_2 pellet and pressed at 100 MPa for 3 min. The superposed pellet placed on a platinum plate was put on an alumina boat and then calcined at 800 °C for 2 h in air and water vapor atmospheres.

After calcination at 800 °C in air atmosphere, the $BaCO_3$ slab was split off from the TiO_2 slab and no compounds were detected on the TiO_2 slab and under the $BaCO_3$ slab. Fig. 10 shows the photograph and XRD patterns of the pellet after the calcination in water vapor atmosphere. In water vapor atmosphere, $BaCO_3$ on the TiO_2 slab spread over the platinum plate as well as the side of the TiO_2 slab after calcination and the $BaCO_3$ slab could not be observed anymore. $BaCO_3$ remained on the TiO_2 slab and was detected on the side of the TiO_2 slab. A small amounts of $Ba(OH)_2{\cdot}8H_2O$ and Ba_2TiO_4 were also detected on the side of TiO_2. Furthermore, it was confirmed that $BaCO_3$ was deposited on the platinum plate. $BaCO_3$ on the platinum plate must be formed by the carbonation of barium hydroxide or barium oxide after the calcination. Thus, gas-phase transport of barium component was clearly observed in water vapor atmosphere.

If the accelerated effects on the formation of $MTiO_3$ by solid-state reactions are determined by a rapid gas-phase transport process in water vapor atmosphere, the gas-phase transport must be faster than the observed reaction rate. In accordance with the Refs. [28,29], a rough estimate of the mass flux of barium, J_g, through the gas-phase can be obtained by means of Fick's law as follows:

$$J_g = -D \cdot \frac{dC}{dx} \approx \frac{D\Delta p}{\lambda RT} \quad (9)$$

where D represents the diffusion coefficient of $Ba(OH)_2$, Δp the variation of $Ba(OH)_2$ partial pressure through the mean free path λ of $Ba(OH)_2$ in a gas-phase, R the gas constant, and T the absolute temperature. The diffusion coefficient of $Ba(OH)_2$ in water vapor atmosphere can be calculated from the kinetic theory of gases to be $\approx 0.32\ cm^2/s$ at 800 °C. Taking $\Delta p = 9.2 \times 10^{-6}$ atm and $\lambda = 0.14\ \mu m$, the gas-phase flux is $\approx 2.5 \times 10^{-6}\ mol/(cm^2\ s)$. The growth rate of $BaTiO_3$ particles calculated from the previous paper[14] is $\approx 3.5 \times 10^{-9}$ cm/s. It can be concluded that the gas-phase transport of $Ba(OH)_2$ is faster than the growth rate of $BaTiO_3$ particles. Thus, barium component might be efficiently supplied to the TiO_2 particle surface in water vapor atmosphere, despite the starting mixture containing coarse particles of $BaCO_3$. Therefore, the gas-phase transport of $M(OH)_2$ would became important for the formation of $MTiO_3$ by solid-state reactions in water vapor atmosphere, and then the difference of acceleration effects on the formation of $MTiO_3$ phases would be strongly dependent on the difference of the vapor pressure of alkaline-earth hydroxides in water vapor atmosphere.

In the previous paper,[14] we found that the formation kinetics of $BaTiO_3$ by calcination of the mixtures of $BaCO_3$ and rutile type TiO_2 followed the Valensi–Carter equation,[34,35] even in water vapor atmosphere. This result suggested that the reaction proceeded by a diffusion controlled process. It is commonly accepted that the formation of $BaTiO_3$ occurs by coupled parallel diffusion of Ba^{2+} and O^{2-} ions from the $BaCO_3/BaTiO_3$ interface to the $BaTiO_3/TiO_2$ interface through the perovskite lattice.[36–38] In addition, it is well known that the $BaTiO_3$ powders prepared by hydrothermal method contain a large amount of protons which are incorporated in the oxygen sublattice as a hydroxyl ions with an effective positive charge. The incorporation of protons in the perovskite lattice might be also formed by solid-state reactions in water vapor atmosphere, and the formation of barium and titanium vacancies with negative charge as compensating defects is required.[39] It is also well known that sintering of $BaTiO_3$ in reducing atmosphere forms O^{2-} ion vacancy ($BaTiO_{3-x}$) with a valence reduction of titanium from Ti^{4+} into Ti^{3+}. In water vapor atmosphere that gives a reducing atmosphere compared with in air atmosphere, O^{2-} ion vacancy with the reduction of titanium ion might be formed in the $BaTiO_3$ structure.

Thus, the accelerated formation of $BaTiO_3$ and the other $MTiO_3$ can be explained by vacancy mechanism for solid-state diffusion. It is considered that the formation of $MTiO_3$ in water vapor atmosphere is still controlled by solid-state diffusion, though the lattice defect concentration is increased and the solid-state diffusion in $MTiO_3$ is enhanced.

4. Conclusions

In the present study, alkaline-earth titanates, $MTiO_3$ (M = Mg, Ca, Sr and Ba), were prepared by solid-state reactions in air and water vapor atmospheres. The formation of $MTiO_3$ was accelerated by water vapor but the acceleration effect by water vapor differed considerably depending on alkaline-earth ions. Water vapor atmosphere gave the most effective influence on the formation of $BaTiO_3$, whereas it gave the least influence on that of $MgTiO_3$ among the four kinds of $MTiO_3$ formation. The difference in its effect might be mainly attributed to the vapor pressure of $M(OH)_2$. Vapor pressure of $Ba(OH)_2$ is 3–6 orders of magnitude higher than the vapor pressure of the other hydroxides. Accordingly, gas-phase transport of $Ba(OH)_2$ may be efficiently occurred in water vapor atmosphere.

Acknowledgement

This work was partly supported by the Sasakawa Scientific Research Grant from The Japan Science Society.

References

1. Phule PP, Risbud SH. Low-temperature synthesis and processing of electronic materials in the BaO–TiO_2 system. *J Mater Sci* 1990;**25**:1169–83.
2. Dawson WJ. Hydrothermal synthesis of advanced ceramic powders. *Ceram Bull* 1988;**67**:1673–8.
3. Hennings DFK, Schreinemacher BS, Schreinemacher H. Solid-state preparation of $BaTiO_3$-based dielectrics, using ultrafine raw materials. *J Am Ceram Soc* 2001;**84**:2777–82.
4. Buscaglia MT, Bassoli M, Buscaglia V, Alessio R. Solid-state synthesis of ultrafine $BaTiO_3$ powders from nanocrystalline $BaCO_3$ and TiO. *J Am Ceram Soc* 2005;**88**:2374–9.
5. Buscaglia MT, Bassoli M, Buscaglia V, Vormberg R. Solid-state synthesis of nanocrystalline $BaTiO_3$: reaction kinetics and powder properties. *J Am Ceram Soc* 2008;**91**:2862–9.
6. Wang TX, Chen WW. Solid phase preparation of submicron-sized $SrTiO_3$ crystallites from SrO_2 nanoparticles and TiO_2 powders. *Mater Lett* 2008;**62**:2865–7.
7. Gomez-Yañez C, Benitez C, Balmori-Ramirez H. Mechanical activation of the synthesis reaction of $BaTiO_3$ from a mixture of $BaCO_3$ and TiO_2 powders. *Ceram Int* 2000;**26**:271–7.
8. Berbenni V, Marini A, Bruni G. Effect of mechanical milling on solid state formation of $BaTiO_3$ from $BaCO_3$–TiO_2 (rutile) mixtures. *Thermochim Acta* 2001;**374**:151–8.
9. Yanagawa R, Senna M, Ando C, Chazono H, Kishi H. Preparation of 200 nm $BaTiO_3$ particles with their tetragonality 1.010 via a solid-state reaction proceeded by agglomeration-free mechanical activation. *J Am Ceram Soc* 2007;**90**:809–14.
10. Kong LB, Ma J, Huang H, Zhang RF, Que WX. Barium titanate derived from mechanochemically activated powder. *J Alloys Comp* 2002;**337**:226–30.
11. Baek JG, Isobe T, Senna M. Mechanochemical effects on the precursor formation and microwave dielectric characteristics of $MgTiO_3$. *Solid State Ionics* 1996;**90**:269–79.
12. Evans IR, Howard JAK, Sreckovic T, Ristic MM. Variable temperature in situ X-ray diffraction study of mechanically activated synthesis of calcium titanate, $CaTiO_3$. *Mater Res Bull* 2003;**38**:1203–13.
13. Berbenni V, Marini A, Bruni G. Effect of mechanical activation on the preparation of $SrTiO_3$ and Sr_2TiO_4 ceramics from the solid state system $SrCO_3$–TiO_2. *J Alloys Compd* 2001;**329**:230–8.
14. Kozawa T, Onda A, Yanagisawa K. Accelerated formation of barium titanate by solid-state reaction in water vapour atmosphere. *J Eur Ceram Soc* 2009;**29**:3259–64.
15. Kozawa T, Onda A, Yanagisawa K. Accelerated formation of β-dicalcium silicate by solid-state reaction in water vapor atmosphere. *Chem Lett* 2009;**38**:476–7.
16. Wechsler BA, Von Dreele RB. Structure refinements of Mg_2TiO_4, $MgTiO_3$ and $MgTi_2O_5$ by time-of-flight neutron powder diffraction. *Acta Crystallogr* 1989;**B45**:542–9.
17. Liao J, Senna M. Crystallization of titania and magnesium titanate from mechanically activated $Mg(OH)_2$ and TiO_2 gel mixture. *Mater Res Bull* 1995;**30**:385–92.
18. Sreedhar K, Pavaskar NR. Synthesis of $MgTiO_3$ and $Mg_4Nb_2O_9$ using stoichiometrically excess MgO. *Mater Lett* 2002;**53**:452–5.
19. MacIntire WH, Stansel TB. Steam catalysis in calcinations of dolomite and limestone fines. *Ind Eng Chem* 1953;**45**:1548–55.
20. Burnham AK, Stubblefield CT, Campbell JH. Effects of gas environmental reactions in Colorado oil shale. *Fuel* 1980;**59**:871–7.
21. Wang Y, Thomson WJ. The effects of steam and carbon dioxide on calcite decomposition using dynamic X-ray diffraction. *Chem Eng Sci* 1995;**50**:1373–82.
22. Agnew J, Hampartsoumian E, Jones JM, Nimmo W. The simultaneous calcination and sintering of calcium based sorbents under a combustion atmosphere. *Fuel* 2000;**79**:1515–23.
23. Hungría T, Lisoni JG, Castro A. $Sr_3Ti_2O_7$ Ruddlesden–Popper phase synthesis by milling routes. *Chem Mater* 2002;**14**:1747–54.
24. Liu Y, Lu T, Xu M, Zhoun L. Formation mechanisms of platelet $Sr_3Ti_2O_7$ crystals synthesized by the molten salt synthesis method. *J Am Ceram Soc* 2007;**90**:1774–9.
25. Carter RE. Mechanism of solid-state reaction between magnesium oxide and aluminum oxide and between magnesium oxide and ferric oxide. *J Am Ceram Soc* 1961;**44**:116–20.
26. Pettit FS, Randklev EH, Felten EJ. Formation of $NiAl_2O_4$ by solid state reaction. *J Am Ceram Soc* 1966;**49**:199–203.

27. Okada H, Kawakami H, Hashiba M, Miura E, Nurishi Y, Hibino T. Effect of physical nature of powders and firing atmosphere on $ZnAl_2O_4$ formation. *J Am Ceram Soc* 1985;**68**:58–63.
28. Buscaglia V, Buscaglia MT, Giordano L, Martinelli A, Viviani M, Bottino C. Growth of ternary oxides in the Gd_2O_3–Fe_2O_3 system. A diffusion couple study. *Solid State Ionics* 2002;**146**:257–71.
29. Ubaldini A, Buscaglia V, Uliana C, Costa G, Ferretti M. Kinetics and mechanism of formation of barium zirconate from barium carbonate and zirconia powders. *J Am Ceram Soc* 2003;**86**:19–25.
30. L'vov BV. Mechanism of thermal decomposition of alkaline-carbonates. *Thermochim Acta* 1997;**303**:161–70.
31. Alexander CA, Ogden JS, Levy A. Transpiration study of magnesium oxide. *J Chem Phys* 1963;**39**:3057–60.
32. Matsumoto K, Sata T. A study of the calcium oxide-water vapor system by means of the transpiration method. *Bull Chem Soc Jpn* 1981;**54**:674–7.
33. Ali (Basu) M, Mishra R, Kerkar AS, Bharadwaj SR, Das D. Gibbs energy of formation of $Ba(OH)_2$ vapor species using the transpiration technique. *J Nucl Mater* 2001;**289**:243–6.
34. Carter RE. Kinetic model for solid-state reactions. *J Chem Phys* 1961;**34**:2010–5.
35. Frade JR, Cable M. Reexamination of the basic theoretical model for the kinetics of solid-state reaction. *J Am Ceram Soc* 1992;**75**: 1949–57.
36. Graff A, Senz S, Voltzke D, Abicht H-P, Hesse D. Microstructure evolution during $BaTiO_3$ formation by solid-state reactions on rutile single crystal surfaces. *J Eur Ceram Soc* 2005;**25**:2201–6.
37. Lotnyk A, Senz S, Hesse D. Formation of $BaTiO_3$ thin films from (1 1 0) TiO_2 rutile single crystals and $BaCO_3$ by solid state reactions. *Solid State Ionics* 2006;**177**:429–36.
38. Lotnyk A, Senz S, Hesse D. Thin-film solid-state reactions of solid $BaCO_3$ and BaO vapor with (1 0 0) rutile substrates. *Acta Mater* 2007;**55**:2671–81.
39. Hennings DFK, Metzmacher C, Schreinemacher BS. Defect chemistry and microstructure of hydrothermal barium titanate. *J Am Ceram Soc* 2001;**84**:179–82.